● RESEARCH ARTICLE

MicroRNA-181c provides neuroprotection in an intracerebral hemorrhage model

Xi Lu, Hui-Yuan Zhang, Zhi-Yi He[*]

First Affiliated Hospital of China Medical University, Shenyang, Liaoning Province, China

Graphical Abstract

Neuroprotective mechanisms of miR-181c in intracerebral hemorrhage

Correspondence to:
Zhi-Yi He, PhD,
hezhiyi0301@sina.com.

orcid:
0000-0002-0995-0294
(Zhi-Yi He)
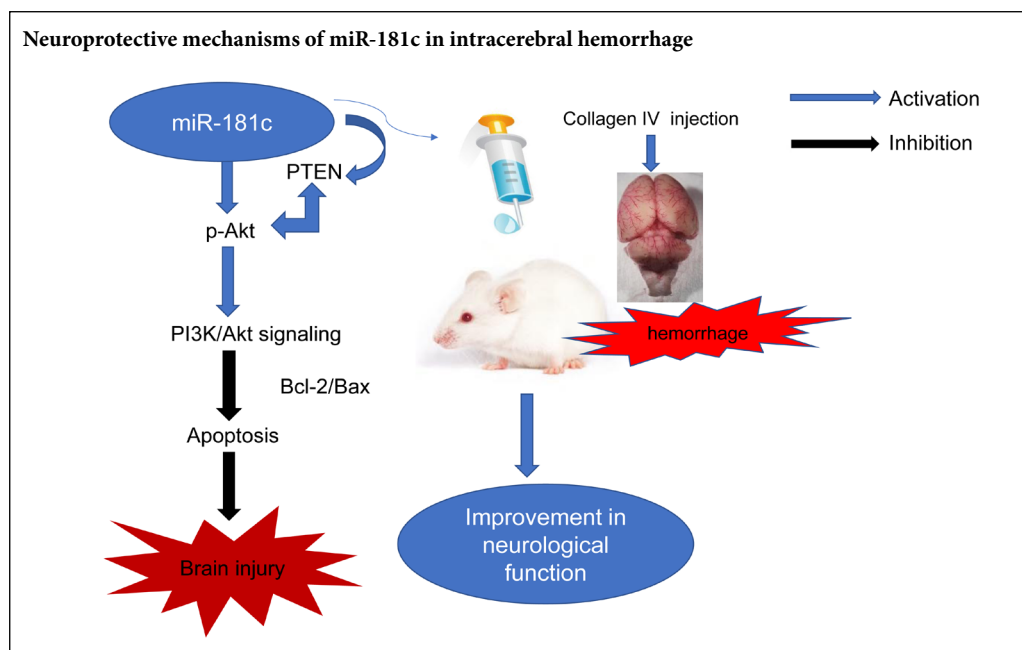
Abstract

Apoptosis is an important factor during the early stage of intracerebral hemorrhage. MiR-181c plays a key regulatory role in apoptosis. However, whether miR-181c is involved in apoptosis of prophase cells after intracerebral hemorrhage remains unclear. Therefore, *in vitro* and *in vivo* experiments were conducted to test this hypothesis. *In vivo* experiments: collagenase type VII was injected into the basal ganglia of adult Sprague-Dawley rats to establish an intracerebral hemorrhage model. MiR-181c mimic or inhibitor was injected *in situ* 4 hours after intracerebral hemorrhage. Neurological functional defects (neurological severity scores) were assessed 1, 7, and 14 days after model establishment. Terminal deoxynucleotidyl transferase-mediated deoxyuridine triphosphate nick-end labeling and western blot assay were conducted 14 days after model establishment. *In vitro* experiments: PC12 cells were cultured under oxygen-glucose deprivation, and hemins were added to simulate intracerebral hemorrhage *in vitro*. MiR-181c mimic or inhibitor was added to regulate miR-181c expression. 3-(4,5-Dimethylthiazol-2-yl)-2,5-diphenyltetrazolium bromide assay, luciferase reporter system, and western blot assay were performed. Experimental results revealed differences in miR-181c expression in brain tissues of both patients and rats with cerebral hemorrhage. In addition, *in vitro* experiments found that miR-181c overexpression could upregulate the Bcl-2/Bax ratio to inhibit apoptosis, while inhibition of miR-181c expression could reduce the Bcl-2/Bax ratio and aggravate apoptosis of cells. Regulation of apoptosis occurred through the phosphoinositide 3 kinase (PI3K)/Akt pathway by targeting of phosphatase and tensin homolog deleted on chromosome ten (PTEN). Higher miR-181c overexpression correlated with lower neurological severity scores, indicating better recovery of neurological function. In conclusion, miR-181c affects the prognosis of intracerebral hemorrhage by regulating apoptosis, and these effects might be directly mediated and regulated by targeting of the PTEN\PI3K/Akt pathway and Bcl-2/Bax ratio. Furthermore, these results indicated that miR-181c played a neuroprotective role in intracerebral hemorrhage by regulating apoptosis of nerve cells, thus providing a potential target for the prevention and treatment of intracerebral hemorrhage. Testing of human serum was authorized by the Ethics Committee of China Medical University (No. 2012-38-1) on February 20, 2012. The protocol was registered with the Chinese Clinical Trial Registry (Registration No. ChiCTR-COC-17013559). The animal study was approved by the Institutional Animal Care and Use Committee of China Medical University (approval No. 2017008) on March 8, 2017.

Key Words: apoptosis; Bcl-2/Bax; intracerebral hemorrhage; miR-181c; nerve cells; neurological function; neuroprotection; PTEN; regulation

Chinese Library Classification No. *R453; R364; R363*

Introduction

Intracerebral hemorrhage (ICH) is the main cause of high morbidity and mortality in patients with cerebrovascular rupture, thus representing a major public health concern (Qureshi et al., 2009; Chang et al., 2019; Li et al., 2019). Injuries associated with ICH involve blood-brain barrier disruption, cerebral edema, inflammation, autophagy, microglial activation, astrocyte proliferation, and neuronal death (Keep et al., 2012; Yuan et al., 2018). Apoptosis is considered to be the major mechanism leading to cell injury after ICH (Ducruet et al., 2009). Neuronal apoptosis occurs following ICH as a result of hypoxia, inflammation, and oxidation products. Recent studies revealed that inhibition of neuronal apoptosis may improve ICH prognosis (Sansing et al., 2016; Zille et al., 2017). Two distinct apoptotic pathways exist, including the intrinsic/mitochondrial pathway and extrinsic/death receptor pathway (Elmore, 2007). Mitochondrial dysfunction is a critical element which activated the intrinsic apoptosis pathway (Chun et al., 2015; Liu et al., 2015). In addition, many other molecular signaling pathways may lead to further neuronal injuries following ICH (Selim, 2009). As one of the signaling pathways for cell survival, phosphoinositide 3 kinase (PI3K)/Akt signal transduction is the major TrkB-mediated survival pathway that promotes neuronal survival and protects against apoptosis (Li et al., 2013). Activated Akt maintains mitochondrial integrity by antagonizing the pro-apoptotic actions of Bcl-2 family members Bad and Bax (Jia et al., 2016). However, the precise mechanism for Bcl-2 family members in neuronal apoptotic functions underlying ICH remains unclear. Further elucidation of mechanisms by which ICH-induced apoptosis occurs may facilitate the development of significant treatments or preventive strategies for ICH.

A set of candidate markers for this condition has been identified. Notably, some of the most promising biomarkers are microRNAs (miRNAs), which target specific messenger RNAs for promotion or inhibition of translation through base pairing to partially or fully complementary sites (Carthew et al., 2009). Increasing evidence indicates that miRNAs are involved in the regulation of pathological and physiological processes of cerebral diseases (Dai et al., 2015; Altintas et al., 2016). miRNA expression patterns were recently studied in the human Alzheimer's disease brain; notably, the level of miR-206, which acts as a brain-derived neurotrophic factor, was markedly increased in Alzheimer's disease mice (Lee et al., 2012). In addition, changes in some miRNAs were observed in a mouse stroke model, and miRNA modulation was confirmed to have neuroprotective potential under oxygen-glucose deprivation conditions *in vitro* (Guo et al., 2013; Ning et al., 2017; Zhang et al., 2018). Among many miRNAs, miR-181c has been identified to act as an important factor in a series of essential biological processes, including various types of apoptosis, but especially mitochondrial apoptosis. Previous findings suggest that miR-181c acts as an important factor in cardiac cell growth and the invasive behavior of tumors. Moreover, previous studies have reported the importance of miR-181c in pancreatic ductal adenocarcinoma, while others showed the anti-tumor function of miR-181c in ovarian cancer cells (Huang et al., 2015; He et al., 2016; Zhao et al., 2016). In addition, recent studies have found that miR-181c may have a profound effect on neurons, cell proliferation, differentiation and apoptosis (Ma et al., 2016). However, the function of miR-181c in ICH is unclear.

Therefore, the purpose of this study was to investigate the effects of miR-181c on nerve cells under ICH, and to identify mechanisms by which miR-181c may ameliorate cerebral cell apoptosis and apoptosis-related gene expression.

Materials and Methods

ICH patient collection *in vivo*

Use of human blood for the study protocol was approved by the Ethics Committee of China Medical University, China (No. 2012-38-1) on February 20, 2012, and all patient family members provided signed informed consent. Patients with acute spontaneous ICH (*n* = 22) were enrolled between October 2016 and September 2017 from the Department of Neurology, the First Affiliated Hospital of China Medical University (Shenyang, China). Inclusion criteria for clinical samples have been previously described, and were as follows: (1) patients aged ≥ 18 years; (2) blood samples of ICH patients (Morotti et al., 2016) obtained within 72 hours after symptoms appeared. Exclusion criteria were secondary ICH (including hemorrhage resulting from underlying structural lesions, hemorrhage infarction, or use of a thrombolytic agent), a recent stroke (within 3 months), or refusal to participate (Wang et al., 2016a, b). Healthy controls (*n* = 18) were recruited from the Physical Examination Department of the First Affiliated Hospital of China Medical University. None of the controls showed evidence of stroke or other neurological diseases. Control participants with tumors, autoimmune diseases, liver ailments, nephrosis, or hematological diseases were excluded. All data assembled at admission are listed in **Table 1**. Each patient's hemorrhagic mass was detected by non-contrast computed tomography (CT). CT images were measured by three doctors blinded to the experimental design.

Real-time polymerase chain reaction quantification of miR-181c levels in human plasma

Blood samples were obtained in centrifuge tubes and centrifuged at 3000 × *g* for 5 minutes. Blood concentrations of miR-181c in ICH and control patients were measured by real-time polymerase chain reaction (RT-PCR). Total RNA was detected by adding 750 μL of TRIzol reagent (Molecular Research Center, Cincinnati, OH, USA) and 20 μL of glacial acetic acid to 200 μL of blood sample; 800 ng of RNA was reverse transcribed using SuperScript III Reverse Transcriptase (Epicentre Biotechnologies, Madison, WI, USA) with miRNA RT primer (Bioligo, Shanghai, China). Expression of mature human miRNAs was detected by a stem-loop RT-PCR system using an Agilent 2100 Bioanalyzer (Agilent Technologies, Santa Clara, CA, USA). Relative expression was calculated with the comparative threshold cycle (Ct)

Table 1 Demographic and clinical data

Variable	Cases	Controls	*P*-value
Age (mean ± SD, yr)	56±13	53±11	0.870
Male [*n*(%)]	15(68)	10(56)	0.317
Medical history [*n*(%)]			
Hypertension	12(63)	10(56)	0.670
Previous intracerebral hemorrhage	3(14)	1(6)	0.317
Ischemic stroke	5(22)	3(17)	0.480
Diabetes mellitus	10(45)	9(50)	0.819
Medication [*n*(%)]			
Antihypertensive therapy	10(45)	10(56)	1.000
Antiplatelet therapy	5(22)	3(17)	0.480
Warfarin anticoagulation	0	0	–
Statin therapy	5(22)	3(17)	0.480
Admission clinical data [median (IQR), mmHg]			
Systolic blood pressure	162(134, 187)	132(120, 156)	0.407
Diastolic blood pressure	96(78, 102)	84(68, 98)	0.637

using the following formula: relative expression = $2^{-\Delta\Delta CT}$, and was standardized to expression of the control U6. Primers used for RT-PCR are listed in **Table 2**.

Animal preparation and collagenase VII-induced hemorrhage *in vivo*

All animal procedures followed the United States National Institutes of Health (NIH) Guide for the Care and Use of Laboratory Animals (NIH Publication No. 85-23, revised 1996). The study was approved by the Institutional Animal Care and Use Committee of China Medical University (approval No. 2017008) on March 8, 2017. Seventy-two male Sprague-Dawley rats aged 8–10 weeks and weighing 250–300 g were purchased from Liaoning Chang Sheng Biotechnology Co., Ltd. [Benxi, China; Approval No. SCXK(Liao)-2015-0001]. Animals were raised in a specific-pathogen-free facility and allowed free access to food and water. The rat ICH model, established on the basis of Rosenberg's technique (Rosenberg et al., 1990), was performed by stereotactic administration of 0.5 U collagenase type VII (Gibco, Sidney, Australia) in saline 2 μL at the injection site as follows: 3.0 mm left lateral to the midline, 0.2 mm posterior to bregma, and 6.0 mm in depth below the skull, which is the location of the basal ganglia.

Rats were randomly divided into two groups and the following subgroups. (1) miR-181c groups (*n* = 16): eight rats underwent collagenase VII-induced ICH surgery, while the remaining eight rats received saline injection. All rats were sacrificed after 24 hours. These two groups of brains were divided into lateral and contralateral hemispheres, and brain tissue adjoining the surgery location was harvested similarly in each hemisphere and stored at –80°C until use. Tissue adjoining the hematomal mass was used for western blot assay and quantitative RT-PCR. (2) Experimental groups (*n* = 56): (a) ICH group (*n* = 8), rats underwent ICH surgery; (b) Sham group (*n* = 8), rats underwent ICH surgical procedures but with normal saline injection instead of collagenase

type VII; (c) miR-181c mimic group (*n* = 8), rats underwent ICH surgery and received miR-181c mimic through intracerebral injection; (d) miR-181c inhibitor group (*n* = 8), rats underwent ICH surgery and received miR-181c inhibitor via intracerebral injection; (e) mimic negative group (*n* = 8), rats underwent ICH surgery and received mimic via intracerebral injection; (f) inhibitor negative group (*n* = 8), rats underwent ICH surgery and received inhibitor via intracerebral injection; and (g) control group, the remaining eight male rats underwent no procedures. All experimental data were collected and analyzed by an investigator who was blinded to the grouping of rats.

Neurological deficiency assessment of ICH rats *in vivo*

Neurological severity scores were used for neurological deficiency assessment (Schallert et al., 1997; Li et al., 2000; Chen et al., 2001). Rats from the ICH group were sacrificed after neurological severity scores were obtained at 1, 7, and 14 days. Analyses were performed by an investigator blinded to the genotypes of ICH-treated rats.

Quantitative RT-PCR of rat brain tissues *in vivo*

MiR-181c expression was examined in tissues adjoining hematomal mass samples by extraction with a miRNeasy Mini Kit (Qiagen, Hilden, Germany), followed by amplification with a GenoExplorer miRNA qRT-PCR kit (GenoSensor Corporation, Tempe, AZ, USA) and miRNA-specific primers (Sangon, Shanghai, China). miR-181c levels were standardized to that of β-actin, as measured with the inverse log of cycle threshold to determine relative fold-change in miR-181c gene expression. Original sequences of miRNAs are shown in **Table 3**.

Table 2 Primer sequence for real-time polymerase chain reaction of human plasma

Gene	Sequence (5′–3′)	Primer size (bp)
Hsa-miR-181c	Forward: GGG GAA CAT TCA ACC TGT CG	20
	Reverse: GTG CGT GTC GTG GAG TCG	
U6	Forward: CGC TTC ACG AAT TTG CGT GTC AT	23
	Reverse: CGC TTC ACG AAT TTG CGT GTC AT	

Table 3 Primer sequence for real-time polymerase chain reaction of brain tissues of rats

Gene	Sequence (5′–3′)	Primer size (bp)
miR-181c-5p	Forward: GTG CAG GGT CCG AGG TAT TC	20
	Reverse: GTG CAG GGT CCG AGG TAT TC	
β-Actin	Forward: GGC CGG ACT CAT CGT ACT CCT GCT T	25
	Reverse: GGC CGG ACT CAT CGT ACT CCT GCT T	

Apoptotic cells in rat brain tissue measured by TUNEL assay *in vivo*

Brains were fixed with 4% paraformaldehyde for 24 hours and dehydrated using 70–100% alcohol. Paraffin-embedded brains were cut into 5-μm sections. Terminal deoxynucleotidyl transferase-mediated deoxyuridine triphosphate nick-end labeling (TUNEL) staining was performed in accordance with the manufacturer's protocols with minor modifications. In brief, slices were washed three times with phosphate-buffered saline, fixed with 4% paraformaldehyde for 30 minutes, incubated in 0.5% Triton X-100 for 5 minutes, and then incubated in TUNEL reaction mixture for 60 minutes at 37°C. Nuclei were stained by 4′,6-diamidino-2-phenylindole (DAPI; 1:2000) for 2 minutes. Stained sections were imaged with an epifluorescence microscope (Olympus, Tokyo, Japan). Nuclei were positively stained (blue), while apoptotic cells appeared brown. Three fields were selected from each section. Numbers of blue/brown cells in each field was counted. Percentage of TUNEL-positive cells was calculated as brown cells/blue cells × 100.

Western blot assay of ICH rat brain tissues *in vivo*

Western blot assay was performed to measure levels of proteins of interest. Specimens were subjected to sodium dodecyl sulfate-polyacrylamide gel electrophoresis (SDS-PAGE), and transferred to a polyvinylidene difluoride membrane by a transfer apparatus at 300 mA for 2.5 hours. The membrane was blocked with 5% non-fat milk before incubation in 1% bovine serum albumin solution containing the following primary rabbit-anti-rat polyclonal antibodies overnight at 4°C: anti-phosphatase and tensin homolog deleted on chromosome ten (PTEN) (1:500), anti-Akt (1:500), anti-p-Akt (1:500), anti-Bcl-2 (1:500), anti-Bax (1:500), anti-cleaved caspase-3 (1:500) and anti-β-actin (1:1000). All primary antibodies were obtained from Wanleibio (Shenyang, China). After washes with Tris-buffered saline containing Tween, membranes were cultured with secondary horseradish peroxidase-conjugated goat anti-rabbit IgG (1:5000; Bioss, Woburn, MA, USA) for 45 minutes at 37°C and detected with an enhanced chemiluminescence system. ImageJ software (NIH, Bethesda, MD, USA) was used to analyze optical densities of immunoreactive bands. Protein expression was normalized to that of the loading control (β-actin).

Cell culture and transfection in ICH models *in vitro*

The rat pheochromocytoma cell (PC12) line (Institute of Biophysics, Chinese Academy of Sciences, Beijing, China), which is commonly used as an *in vitro* model of neuronal function and differentiation, was incubated in RPMI 1640 (Gibco) media supplemented with 10% fetal bovine serum (Gibco). Samples were cultured in a chamber with 5% CO_2 at 37°C. Cells were seeded in six-well plates and transfected with miR-181c mimic, miR-181c inhibitor, mimic negative, inhibitor negative, or control using Lipofectamine 2000 (Invitrogen, Carlsbad, CA, USA) for 24 hours, according to the manufacturer's protocol. miR-181c mimic and inhibitor were synthesized by Shanghai Gene Pharma Company (Shanghai, China); sequences are shown in **Table 4**. Transfected cells were used for further analysis. To simulate ICH, cells were treated with glucose-free RPMI and exposed to 10 μM hemin (heme with a chloride ligand released from hemoglobin in blood to outside vessels, whereby it plays a key role in ICH; MedChemExpress, Shanghai, China). Cells were then incubated in 1% O_2, 5% CO_2, and 94% N_2 at 37°C to induce ICH for 4 hours. Cells in normoxia throughout experiments were used as the control group.

Table 4 Sequences of miR-181c mimic, inhibitor and negative controls

Name	Sequences (5′–3′)	Primer size (bp)
miR-181c mimic	Forward: AAC AUU CAA CCU GUC GGU GAG U	22
	Reverse: UCA CCG ACA GGU UGA AUG UUU U	22
miR-181c inhibitor	Forward: ACU CAC CGA CAG GUU GAA UGU U	22
Mimic negative control	Forward: UUC UCC GAC GUG UCA CGU TT	23
	Reverse: ACG UGA CAC GUU CGG AGA ATT	23
Inhibitor negative control	Forward: CAG UAC UUU UGU AGU ACA A	21

Dual luciferase reporter assay for cells *in vitro*

Wild-type PTEN 3′UTR (wt-PTEN) including potential miR-181c binding sites was amplified by specific primers using genomic DNA as a template, and then inserted downstream of the luciferase gene sequence in the pUM-T simple vector (BioTeke, Winooski, VT, USA). Mutant PTEN 3′UTR (mut-PTEN) was generated by PCR. All vectors were confirmed by DNA sequencing. Cells were plated in 96-well plates in five replicates. For transfection, 2 μL of 20 μM miR-181c mimic or inhibitor (**Table 4**) and 150 ng of reporter plasmid (either wt-PTEN or mut-PTEN) were mixed with 2 μL of Lipofectamine 2000. Briefly, luciferase activity was assessed using a Dual-Luciferase Assay System (Promega, Madison, WI, USA) and normalized to Renilla activity (Genechem, Shanghai, China).

Cellular apoptosis analyzed by MTT assay *in vitro*

A 3-(4,5-dimethylthiazol-2-yl)-2,5-diphenyltetrazolium bromide (MTT) assay was performed to determine the extent of cellular apoptosis. PC12 cells were plated in a 96-well plate (200 μL/well) at a density of 4×10^3 cells per well. After 24 hours, the cells were treated with hemin 10 μM. Following incubation in 1% O_2, 5% CO_2, and 94% N_2 at 37°C for 4 hours, 20 μL of 0.5 mg/ml MTT reagent (Beijing Solarbio Science & Technology Co., Ltd.) was added to each well for 4 hours. The medium was then removed and 150 μL dimethyl sulfoxide was added to dissolve the formazan crystals. Finally, absorbance values at 570 nm were determined using a spectrophotometer.

Western blot assay of cells in ICH models *in vitro*
PC12 cells were lysed in radio immunoprecita-tion assay buffer (Beyotime, Beijing, China) containing 1% phenyl-methylsulfonyl fluoride (Solarbio, Guangzhou, China) for 30 minutes. Lysates were centrifuged at $12,000 \times g$ at 4°C for 15 minutes. Protein concentrations were determined using a bicinchoninic acid protein kit (Thermo Fisher Scientific, Waltham, MA, USA). Cell lysates were separated via 5–15% SDS-PAGE electrophoresis. Proteins were transferred to polyvinylidene difluoride membranes, which were incubated in 1% bovine serum albumin solution with the following primary rabbit-anti-rat polyclonal antibodies overnight at 4°C: anti-PTEN (1:500), anti-Akt (1:500), anti-p-Akt (1:500), anti-Bcl-2 (1:500), anti-Bax (1:500), an-ti-cleaved caspase-3 (1:500), and anti-β-actin (1:1000). After washes with Tris-buffered saline containing Tween, membranes were cultured with secondary horseradish peroxidase-conjugated goat anti-rabbit IgG (1:5000; Bioss) for 45 minutes at 37°C.

Statistical analysis
All data are expressed as the mean ± standard error of the mean (SEM). Comparisons between multiple groups were tested using one-way analysis of the variance followed by the least significant difference test. All data were analyzed using SPSS 23.0 software (IBM, Armonk, NY, USA) and GraphPad Prism 5.0 software (GraphPad Software, La Jolla, CA, USA). All *in vitro* and *in vivo* assays were repeated at least three times. $P < 0.05$ (two-tailed) was considered statistically significant.

Results

MiR-181c is downregulated in ICH patient plasma and rat ICH model brain tissues *in vivo*
To assess the apoptotic functions of miRNAs after ICH, miR-181c levels were measured in the plasma of ICH patients. A total of 40 blood samples were acquired. RT-PCR analysis suggested that miR-181c levels were downregulated in the serum of ICH patients compared with healthy controls (**Figure 1A**; $P < 0.05$). Furthermore, microarray results suggested that miR-181c was significantly downregulated in the hemorrhagic hemisphere compared with the contralateral hemisphere (**Figure 1B**; $P < 0.05$).

MiR-181c affects PC12 cell apoptosis in response to ICH *in vitro*
In vitro functional assays were performed by transfection of PC12 cells with miR-181c mimic or inhibitor. As a result, transfection of miR-181c mimic dramatically increased expression levels of miR-181c. Moreover, relative levels of miR-181c were significantly decreased after transfection with miR-181c inhibitor. To determine whether miR-181c takes part in ICH-induced apoptosis, we set up overexpression and knockdown systems by transfecting PC12 cells with miR-181c mimic or inhibitor, respectively. Control cells underwent sham transfection and used as normal controls. The results show that the ratio of apoptotic PC12 cells was notably decreased after ICH treatment compared with the control group transfected with miR-181c mimic. However,

transfection with miR-181c inhibitor significantly promoted ICH-induced apoptosis ($P < 0.05$; **Figure 2B**).

Consistent with morphological changes, western blot assay results showed significantly downregulated Bcl-2 expression and markedly increased Bax, cleaved caspase-3, and caspase-3 expression in PC12 cells after ICH treatment. However, Bcl-2 expression was significantly reduced, while Bax and cleaved caspase-3 and caspase-3 expression were increased in PC12 cells treated with miR-181c inhibitor compared with the ICH group. Overexpression of miR-181c markedly promoted Bcl-2 expression and reduced Bax, cleaved caspase-3, and caspase-3 expression. These findings demonstrate that upregulation of miR-181c reverses the ability of PC12 cells to participate in ICH apoptosis.

Moreover, cell viability in the brain was assessed by the MTT assay. As indicated in **Figure 2A** and **B**, the percentage of stained cells was lower in the ICH group compared with the sham group. Forced overexpression of miR-181c suppressed nerve cell apoptosis compared with the ICH group. Subsequently, western blot assay findings revealed that Bcl-2 expression was lower in the ICH group compared with the sham group, and both were reverted in the ICH+miR-181c mimic group. Additionally, cleaved capase-3 and capase-3 were promoted in the ICH group, but were attenuated in the ICH + miR-181c mimic group (**Figure 2C** and **D**). Taken together, such outcomes indicate that miR-181c can effectively inhibit ICH injury *in vivo*.

PTEN is a direct target of miR-181c
To examine which gene was regulated by miR-181c during apoptosis, bioinformatic analysis was carried out using TargetScan and miRDB to obtain putative target genes of miR-181c. The results revealed that human PTEN mRNA contains a potential binding site within the 3′UTR region of miR-181c. Whether this predicted region is actually targeted by miR-181c was evaluated by dual-luciferase reporter assay. When wt-PTEN plasmid was co-transfected with miR-181c inhibitor, the luciferase activity of T293 cells was significantly decreased; whereas, this effect was almost abolished when the PTEN-3′UTR binding site was mutated. In contrast, the promotional effect of miR-181c on luciferase activity was obviously abolished by co-transfection of PTEN-3′UTR-mut in T293 cells (**Figure 3**). These results support the notion that miR-18c directly targets PTEN.

To further verify whether miR-181c regulates endogenous PTEN, the effects of miR-181c on PTEN were explored in rat ICH brain tissues and PC12 cells by western blot assay. As shown in **Figure 4**, endogenous PTEN protein was significantly expressed in ICH brain tissues. Additionally, expression of PTEN protein was significantly reduced in miR-181c mimic-treated PC12 cells, but markedly enhanced in miR-181c-inhibited PC12 cells (**Figure 4A** and **B**).

The PI3K/Akt signaling pathway reportedly plays a key role in nerve cell apoptosis. As revealed in **Figure 4B**, compared with the control group, the level of Akt phosphorylation was inhibited by ICH treatment, and this inhibition was reduced by overexpression of miR-181c. In contrast, miR-181c knock-
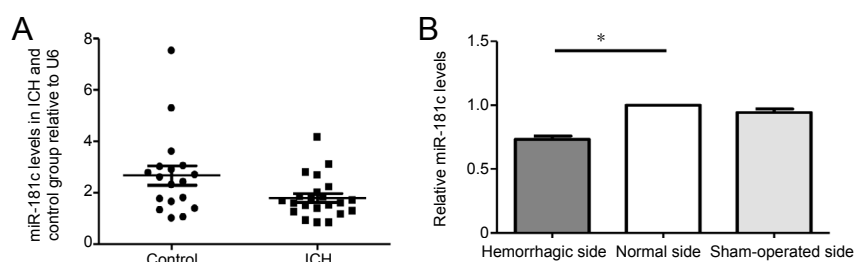
Figure 1 Expression of miR-181c in plasma of ICH patients and tissues of rat ICH models.
(A) Plasma levels of miR-181c in acute hemorrhage patients and controls, as measured by semi-quantitative RT-PCR (n = 18 in the control group, n = 22 in the ICH group), P < 0.05. (B) miR-181c expression after ICH showed a difference between the left hemorrhagic hemisphere and right non-hemorrhagic hemisphere. miR-181c level was decreased in the hemorrhagical mass, as shown by quantitative RT-PCR, while the difference between normal and sham sides had no statistical significance. ∗P < 0.05. Data are expressed as the mean ± SEM (n = 8; one-way analysis of variance followed by the least significant difference test). ICH: Intracerebral hemorrhage; RT-PCR: real-time polymerase chain reaction; SEM: standard error of the mean.
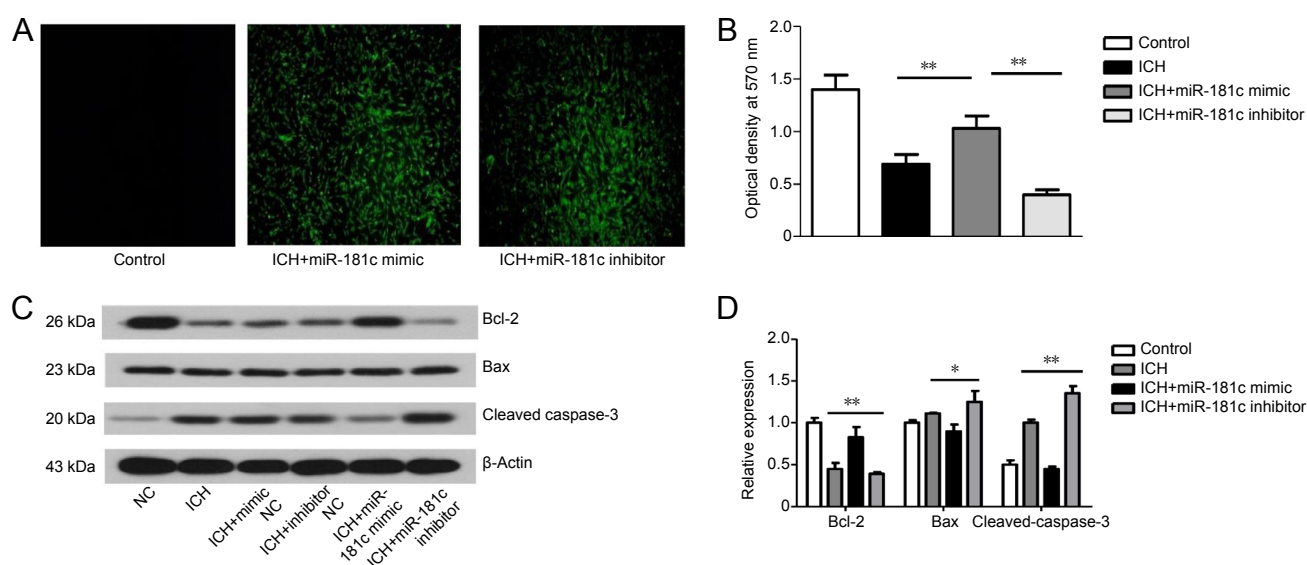
Figure 2 miR-181c reduces ICH-induced apoptosis *in vitro*.
(A) Fluorescence staining images of PC12 cells treated with miR-181c mimic or inhibitor. (B) Cell viability of transfected PC12 cells, as assessed by MTT assay. (C) Representative western blots of Bcl-2, Bax, and cleaved caspase-3. (D) Western blot assay of Bax, Bcl-2, and caspase-3 staining in PC12 cells, including statistics for relative expression. ∗P < 0.05, ∗∗P < 0.01. Data are expressed as the mean ± SEM (n = 3; one-way analysis of variance followed by the least significant difference test). All experiments were conducted at least three times. Bax: Bcl-2 Associated X protein; Bcl-2: B-cell lymphoma-2; ICH: Intracerebral hemorrhage; MTT: 3-(4,5-dimethylthiazol-2-yl)-2,5-diphenyltetrazolium bromide; NC: negative control; SEM: standard error of the mean.
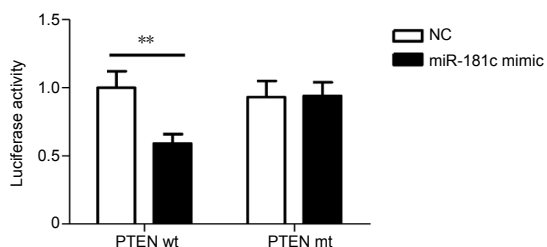
Figure 3 MiR-181c downregulates PTEN by interacting with its 3′UTR.
T293 cells were co-transfected with PTEN-3′UTR-wt or PTEN-3′UTR-mut and miR-181c mimic, and relative luciferase activities were measured. Data are presented as the mean ± SEM (n = 3; one-way analysis of variance followed by the least significant difference test). ∗∗P < 0.01. All experiments were conducted at least three times. mt: Mutant; NC: normal control; PTEN: phosphatase and tensin homolog deleted on chromosome ten; wt: wild-type; SEM: standard error of the mean; UTR: untranslated region.

down reduced p-Akt levels in PC12 cells. These findings indicate that miR-181c may protect against ICH-induced brain cell apoptosis by upregulating PI3K/Akt signaling.

MiR-181c improves neurological deficits of ICH rats and protects against ICH injury *in vivo*

As miR-181c acts as a key suppressor of ICH-induced nerve cell injury *in vitro*, the next step was to explore the effects of miR-181c on nerve cell injury *in vivo*. We assessed neurological function using neurological severity scores. Neurological deficits are one of the most interesting sequelae of ICH, which urgently need to be addressed. Currently, it is feasible to regulate related genes, such as apoptosis-related genes, for future treatments. Our study suggested that miR-181c overexpression could improve neurological function and prognosis; meanwhile an miR-181c inhibitor exacerbated neurological deficits (**Figure 5**, P < 0.05 or P < 0.01). Additionally , western bolt assay findings suggested over expression of miR-

181c could enhance the Bcl-2 expression compared with the ICH group. In contrast, PTEN, cleaved capase-3 and Bax were decreased in the same group, but both were reverted in the miR-181c inhibitor + ICH group ($P < 0.05$; **Figure 5**).

Discussion

ICH, a serious stroke subtype, induces neural cell death and neurological dysfunction (Bimpis et al., 2012; Kuramatsu et al., 2013). Apoptosis acts as a vital factor in ICH (Wang et al., 2014; Kanamaru and Suzuki, 2019). Hence, investigations underlying apoptotic mechanisms will help develop new strategies for the treatment of ICH. Several recent studies showed a correlation between miRNA expression patterns and regulation of pathological and physiological processes of brain diseases; moreover, these findings revealed that upregulated miRNAs could be therapeutic targets for nerve cell apoptosis (Kim et al., 2014; Wang et al., 2016a, b; Zhang et al., 2016). The present study demonstrated that miR-181c overexpression had an anti-apoptotic effect on neurons and improved neurological function in ICH rats.

In previous investigations, miR-181c has mostly been focused on for its role in cancer; for example, miR-181c suppresses the progression of osteosarcoma by targeting SMAD7 and regulating transforming growth factor-β signaling (Fu et al., 2019). In addition, miR-181c was shown to affect estrogen-dependent endometrial carcinoma cell growth by targeting PTEN (Zhuang et al., 2019). Furthermore, miR-181c overexpression facilitated repair of myocardial damage (Ouyang et al., 2012; Wang et al., 2015). However, miR-181c was also shown to exacerbate hypoxia/reoxygenation-induced cardiomyocyte apoptosis by targeting PTPN4, as well as brain injury in acute ischemic stroke (Ma et al., 2016; Ge et al., 2019). As such, the role of miR-181c in ICH was unclear. In this study, we explored the effect of miR-181c on ICH. Our results revealed that miR-181c markedly decreased cellular apoptosis under oxygen-glucose deprivation and hemin treatment, which was used to imitate the ICH microenvironment *in vitro*. Our results indicate that miR-181c mimics can markedly decrease the rate of apoptosis and expression of apoptosis-related proteins induced by ICH, suggesting that miR-181c acts as a protective factor after ICH. We hypothesized that miR-181c could enhance the neuroprotective effects elicited by ICH. Our results showed that miR181c enhanced recovery of neurological function compared with other groups, as evidenced by improved neurological severity scores. Moreover, miR-181c could reduce the number of apoptotic neurons after ICH, and miR-181c overexpression could alleviate injury after transplantation into ICH rats. RT-PCR results revealed decreased miR-181c expression in both ICH patients and ICH rats compared with controls; whereas, miR-181c overexpression was shown to inhibit neuronal apoptosis and protect the brain from injury. However, the precise role of miR-181c in ICH was still unclear.

Our *in vivo* study results revealed that miR-181c noticeably reduced cell death, and regulated the ratio of Bax/Bcl-2 by decreasing Bax and increasing Bcl-2 expression, which are protein kinases primarily involved in controlling mitochondrial apoptosis. The Bax/Bcl-2 ratio is relevant to the regulation of cellular apoptosis (Al-Rasheed et al. 2017). An exciting result in relation to this was that PTEN was predicted to be a target of miR-181c by both Targetscan (www.targetscan.org) and miRDB (www.mirdb.org). In our study, upregulation of miR-181c could decrease PTEN expression in PC12 cells, whereas PTEN was significantly promoted in miR-181c-depleted PC12 cells. A dual-luciferase reporter assay further confirmed that miR-181c directly targeted the PTEN 3′UTR. These findings indicated that PTEN is a functional target gene of miR-181c and contributes to improved neurological function after ICH. Previous studies revealed PTEN to be a lipid phosphatase, the enzymatic activity of which primarily serves to remove phosphate groups from key intracellular phosphoinositide signaling molecules (Zhou et al., 2017; Chen et al., 2018). This enzymatic ability commonly serves to restrict growth and survival signals by inhibiting activity of the PI3k/Akt pathway (Liu et al., 2019). Other studies have shown that PI3k/Akt signaling regulates apoptosis, and PTEN is located upstream of PI3k/Akt (Wang et al., 2013; Guo et al., 2018; Yu et al., 2018; Zhao et al., 2018). We hypothesized that PI3K/Akt signaling pathway activation could be key for miR-181c-induced neuroprotection against ICH. Previous studies demonstrated that PI3K/Akt is an important survival pathway in various neurological disorders (Fukunag et al., 2013; Su et al., 2017). Akt regulates apoptosis, either by transcription or direct phosphorylation. Activated Akt phosphorylates the death promoter Bad to maintain mitochondrial integrity by preventing the inhibition of anti-apoptotic Bcl-2 by Bad (Sussman, 2009). Our results revealed the importance of defining survival pathways that counteract apoptosis induced by ICH. In our study, levels of phosphorylated PI3K/Akt were downregulated after ICH, while upregulation of miR-181c significantly increased PI3K/Akt activity both *in vivo* and *vitro*. Thus, these results indicate that the neuroprotective properties of miR-181c are likely mediated by activation of the PI3K/Akt pathway through targeting of PTEN.

There are several limitations to the present study. First, the rat model of ICH induced by collagenase type VII could not completely simulate the pathological changes of ICH. Moreover, detailed mechanisms involved in post-hemorrhagic neuronal damage in clinical situations include mechanisms beyond a microenvironment of glucose/oxygen deprivation and hemin treatment. Nevertheless, although the PC12 cell line cannot entirely replace primary neurons, it is commonly used as an *in vitro* model of neuronal function and differentiation. Second, there are many potential target genes of miR-181c, and potential properties of miRNAs commonly vary under different conditions. Thus, further studies are necessary to investigate the potential mechanism by which PTEN is involved in the neuroprotection elicited by miR-181c and leads to PI3K/Akt signal transduction in response to ICH.

In summary, miR-181c increased the anti-apoptotic function of cells and improved recovery of neuronal function in acute ICH. Additionally, miR-181c was transported to neurons, which increased their survival rate by targeting PTEN and alleviating activation of the PI3K/Akt pathway. These findings indicate that miR-181c is a potential therapeutic target for ICH.

References

Al-Rasheed N, Faddah LM, Hasan IH, Ali HM, Al-Rasheed N, El Oraby NF, Mohamed MH (2017) Amelioration of panadol-induced nephrotoxicity via down-regulation of Bax/Bcl2 ratio with some antioxidants. Pharmacol Rep 69:1088-1093.

Altintas O, Ozgen Altintas M, Kumas M, Asil T (2016) Neuroprotective effect of ischemic preconditioning via modulating the expression of cerebral miRNAs against transient cerebral ischemia in diabetic rats. Neurol Res 38:1003-1011.

Bimpis A, Papalois A, Tsakiris S, Zarros A, Kalafatakis K, Botis J, Stolakis V, Zissis KM, Liapi C (2012) Activation of acetylcholinesterase after U-74389G administration in a porcine model of intracerebral hemorrhage. Metab Brain Dis 27:221-225.

Carthew RW, Sontheimer EJ (2009) Origins and mechanisms of miRNAs and siRNAs. Cell 136642-123655.

Chang JJ, Armonda R, Goyal N, Arthur AS (2019) Magnesium: Pathophysiological mechanisms and potential therapeutic roles in intracerebral hemorrhage. Neural Regen Res 14:1116-1121.

Chen J, Sanberg PR, Li Y, Wang L, Lu M, Willing AE, Sanchez-Ramos J, Chopp M (2001) Intravenous administration of human umbilical cord blood reduces behavioral deficits after stroke in rats. Stroke 32:2682-2688.

Chen X, Chen P, Chen SS, Ma T, Shi G, Zhou Y, Li J, Sheng L (2018) miR-106b-5p promotes cell cycle progression of malignant melanoma by targeting PTEN. Oncol Rep 39:331-337.

Chun WJ, Nah DY, Bae JH, Chung JW, Lee H, Moon IS (2015) Glucose-insulin-potassium solution protects ventricular myocytes of neonatal rat in an in vitro coverslip ischemia/reperfusion model. Korean Circ J 45:234-241.

Dai A, Liu X, Zhang Y, Han L, Zhu L, Ni H, Chen R, Cao M (2015) Up-regulation of KPNB1 involves in neuronal apoptosis following intracerebral hemorrhage in adult rats. Neurochem Res 40:2177-2187.

Ducruet AF, Zacharia BE, Hickman ZL, Grobelny BT, Yeh ML, Sosunov SA, Connolly ES Jr (2009) The complement cascade as a therapeutic target in intracerebral hemorrhage. Exp Neurol 219:398-403.

Elmore S (2007) Apoptosis: a review of programmed cell death. Toxicol Pathol 35:495-516.

Fu Y, Tang Y, Wang J, Guo Z (2019) MicroRNA-181c suppresses the biological progression of osteosarcoma via targeting SMAD7 and regulating transforming growth factor-beta (tgf-beta) signaling pathway. Med Sci Monit 25:4801-4810.

Fukunaga K, Kawano T (2013) Akt is a molecular target for signal transduction therapy in brain ischemic insult. J Pharmacol Sci 92:317-327.

Ge L, Cai Y, Ying F, Liu H, Zhang D, He Y, Pang L, Yan D, Xu A, Ma H, Xia Z (2019) miR-181c-5p exacerbates hypoxia/reoxygenation-induced cardiomyocyte apoptosis via targeting PTPN4. Oxid Med Cell Longev 2019:1957920.

Guo D, Liu J, Wang W, Hao F, Sun X, Wu X, Bu P, Zhang Y, Liu Y, Liu F, Zhang Q, Jiang F (2013) Alteration in abundance and compartmentalization of inflammation-related miRNAs in plasma after intracerebral hemorrhage. Stroke 44:1739-1742.

Guo D, Xie J, Zhao J, Huang T, Guo X, Song J (2018) Resveratrol protects early brain injury after subarachnoid hemorrhage by activating autophagy and inhibiting apoptosis mediated by the Akt/mTOR pathway. Neuroreport 29:368-379.

He X, Liu Z, Peng Y, Yu C (2016) MicroRNA-181c inhibits glioblastoma cell invasion, migration and mesenchymal transition by targeting TGF-beta pathway. Biochem Biophys Res Commun 469:1041-1048.

Huang P, Ye B, Yang Y, Shi J, Zhao H (2015) MicroRNA-181 functions as a tumor suppressor in non-small cell lung cancer (NSCLC) by targeting Bcl-2. Tumour Biol 36:3381-3387.

Jia Z, Wang J, Shi Q, Liu S, Wang W, Tian Y, Lu Q, Chen P, Ma K, Zhou C (2016) SOX6 and PDCD4 enhance cardiomyocyte apoptosis through LPS-induced miR-499 inhibition. Apoptosis 21:174-183.

Kanamaru H, Suzuki H (2019) Potential therapeutic molecular targets for blood-brain barrier disruption after subarachnoid hemorrhage. Neural Regen Res 14:1138-1143.

Keep RF, Hua Y, Xi G (2012) Intracerebral haemorrhage: mechanisms of injury and therapeutic targets. Lancet Neurol 11:720-731.

Kim JM, Lee ST, Chu K, Jung KH, Kim JH, Yu JS, Kim S, Kim SH, Park DK, Moon J, Ban J, Kim M, Lee SK, Roh JK (2014) Inhibition of Let7c microRNA is neuroprotective in a rat intracerebral hemorrhage model. PLoS One 9:e97946.

Kuramatsu JB, Huttner HB, Schwab S (2013) Advances in the management of intracerebral hemorrhage. J Neural Transm 120 Suppl 1:S35-S41.

Lee ST, Chu K, Jung KH, Kim JH, Huh JY, Yoon H, Park DK, Lim JY, Kim JM, Jeon D, Ryu H, Lee SK, Kim M, Roh JK (2012) miR-206 regulates brain-derived neurotrophic factor in Alzheimer disease model. Ann Neurol 72:269-277.

Li Q, Huai L, Zhang C, Wang C, Jia Y, Chen Y, Yu P, Wang H, Rao Q, Wang M, Wang J (2013) Icaritin induces AML cell apoptosis via the MAPK/ERK and PI3K/AKT signal pathways. Int J Hematol 97:617-23.

Li ZW, Zheng XN, Li P (2019) Time-effect relationship of acupuncture on histopathology, ultrastructure, and neuroethology in the acute phase of cerebral hemorrhage. Neural Regen Res 14:107-113.

Li Y, Chopp M, Chen J, Wang L, Gautam SC, Xu YX, Zhang ZG (2000) Intrastriatal transplantation of bone marrow nonhematopoietic cells improves functional recovery after stroke in adult mice. J Cereb Blood Flow Metab 20:1311-1319.

Liu P, Xie YM, Qian MY (2019) MicroRNA-152-3p negatively regulates schemia-reperfusion induced cardiomyocyte apoptosis by inhibiting PTEN. Int J Clin Exp Med 12:239-250.

Liu P, Zhao H, Wang R, Wang P, Tao Z, Gao L, Yan F, Liu X, Yu S, Ji X, Luo Y (2015) MicroRNA-424 protects against focal cerebral ischemia and reperfusion injury in mice by suppressing oxidative stress. Stroke 46:513-519.

Ma Q, Zhao H, Tao Z, Wang R, Liu P, Han Z, Ma S, Luo Y, Jia J (2016) MicroRNA-181c exacerbates brain injury in acute ischemic stroke. Aging Dis 7:705-714.

Morotti A, Goldstein JN (2016) Diagnosis and management of acute intracerebral hemorrhage. Emerg Med Clin North Am 34:883-899.

Ning X, Tao T, Shen J, Ji Y, Xie L, Wang H, Liu N, Xu X, Sun C, Zhang D, Shen A, Ke K (2017) The O-GlcNAc modification of CDK5 involved in neuronal apoptosis following in vitro intracerebral hemorrhage. Cell Mol Neurobiol 37:527-536.

Ouyang YB, Lu Y, Yue S, Giffard RG (2012) miR-181 targets multiple Bcl-2 family members and influences apoptosis and mitochondrial function in astrocytes. Mitochondrion 12:213-219.

Qureshi AI, Mendelow AD, Hanley DF (2009) Intracerebral haemorrhage. Lancet 373:1632-1644.

Rosenberg GA, Mun-Bryce S, Wesley M, Kornfeld M (1990) Collagenase-induced intracerebral hemorrhage in rats. Stroke 21:801-807.

Sansing LH (2016) Intracerebral hemorrhage. Semin Neurol 36:223-224.

Schallert T, Kozlowski DA, Humm JL, Cocke RR (1997) Use-dependent structural events in recovery of function. Adv Neurol 73:229-238.

Selim M (2009) Deferoxamine mesylate: a new hope for intracerebral hemorrhage: from bench to clinical trials. Stroke 40:S90-91.

Su WS, Wu CH, Chen SF, Yang FY (2017) Transcranial ultrasound stimulation promotes brain-derived neurotrophic factor and reduces apoptosis in a mouse model of traumatic brain injury. Brain Stimul 10:1032-1041.

Sussman MA (2009). Mitochondrial integrity: preservation through Akt/Pim-1 kinase signaling in the cardiomyocyte. Expert Rev Cardiovasc Ther 7:929-938.

Wang G, Jiang X, Pu H, Zhang W, An C, Hu X, Liou AK, Leak RK, Gao Y, Chen J (2013) Scriptaid, a novel histone deacetylase inhibitor, protects against traumatic brain injury via modulation of PTEN and AKT pathway: scriptaid protects against TBI via AKT. Neurotherapeutics 10:124-142.

Wang H, Li J, Chi H, Zhang F, Zhu X, Cai J, Yang X (2015) MicroRNA-181c targets Bcl-2 and regulates mitochondrial morphology in myocardial cells. J Cell Mol Med 19:2084-2097.

Wang J, Zhu Y, Jin F, Tang L, He Z, He Z (2016a) Differential expression of circulating microRNAs in blood and haematoma samples from patients with intracerebral haemorrhage. J Int Med Res 44:419-432.

Wang MD, Wang Y, Xia YP, Dai JW, Gao L, Wang SQ, Wang HJ, Mao L, Li M, Yu SM, Tu Y, He QW, Zhang GP, Wang L, Xu GZ, Xu HB, Zhu LQ, Hu B (2016b) High serum mir-130a levels are associated with severe perihematomal edema and predict adverse outcome in acute ICH. Mol Neurobiol 53:1310-1321.

Wang YC, Zhou Y, Fang H, Lin S, Wang PF, Xiong RP, Chen J, Xiong XY, Lv FL, Liang QL, Yang QW (2014) Toll-like receptor 2/4 heterodimer mediates inflammatory injury in intracerebral hemorrhage. Ann Neurol 75:876-889.

Yu T, Fan Y, Xu Y, Xu L, Xu G, Cao F, Jiang H (2018) Standardized Ginkgo biloba extract EGb 761(R) attenuates early brain injury following subarachnoid hemorrhage via suppressing neuronal apoptosis through the activation of Akt signaling. Biomed Pharmacother 107:329-337.

Yuan ZJ, He XY, Yuan P, Zheng XM, Li XG (2018) Morroniside improves the neurological function in intracerebral hemorrhage rats by inhibiting inflammatory response. Zhongguo Zuzhi Gongcheng Yanjiu 22:1217-1222.

Zhang H, Wang Y, Zhu A, Huang D, Deng S, Cheng J, Zhu MX, Li Y (2016) SUMO-specific protease 1 protects neurons from apoptotic death during transient brain ischemia/reperfusion. Cell Death Dis 7:e2484.

Zhang HY, Wang YZ, He ZY (2018) Glycine-histidine-lysine (GHK) alleviates neuronal apoptosis due to intracerebral hemorrhage via the miR-339-5p/VEGFA pathway. Front Neurosci 12:644.

Zhao D, Chen J, Zhang Y, Liao HB, Zhang ZF, Zhuang Y, Pan MX, Tang JC, Liu R, Lei Y, Wang S, Qin XP, Feng YG, Chen Y, Wan Q (2018) Glycine confers neuroprotection through PTEN/AKT signal pathway in experimental intracerebral hemorrhage. Biochem Biophys Res Commun 501:85-91.

Zhao L, Li Y, Song X, Zhou H, Li N, Miao Y, Jia L (2016) Upregulation of miR-181c inhibits chemoresistance by targeting ST8SIA4 in chronic myelocytic leukemia. Oncotarget 7:60074-60086.
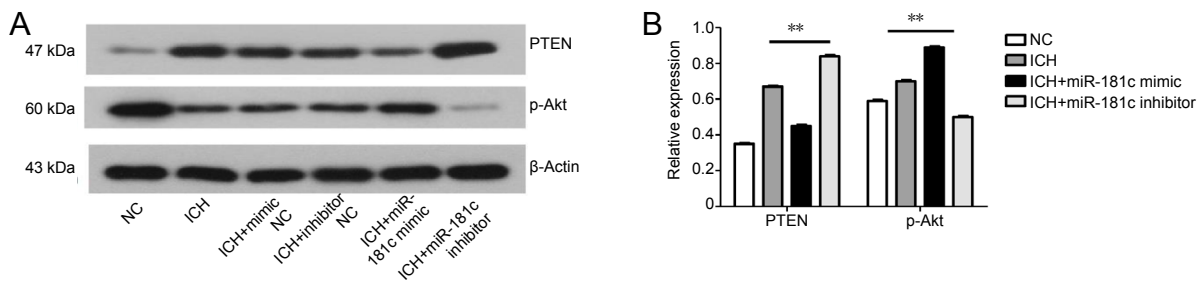
Figure 4 miR-181c reduces PI3K/Akt signaling through targeting on PTEN in an *in vitro* ICH model.
(A) Western blot assay of PTEN and phosphorylated PI3K/Akt in PC12 cells after transfection with either miR-181c inhibitor or miR-181c mimic; β-actin was used as an endogenous control. (B) Western blot assay of PTEN and p-Akt staining in PC12 cells, including statistics for relative expression. ∗∗$P < 0.01$. Data are expressed as the mean ± SEM ($n = 3$; one-way analysis of variance followed by the least significant difference test). All experiments were measured at least three times. ICH: Intracerebral hemorrhage; NC: normal control; p-AKT: phosphorylated Akt; PI3K: phosphoinositide 3 kinase; PTEN: phosphatase and tensin homolog deleted on chromosome ten; SEM: standard error of the mean.
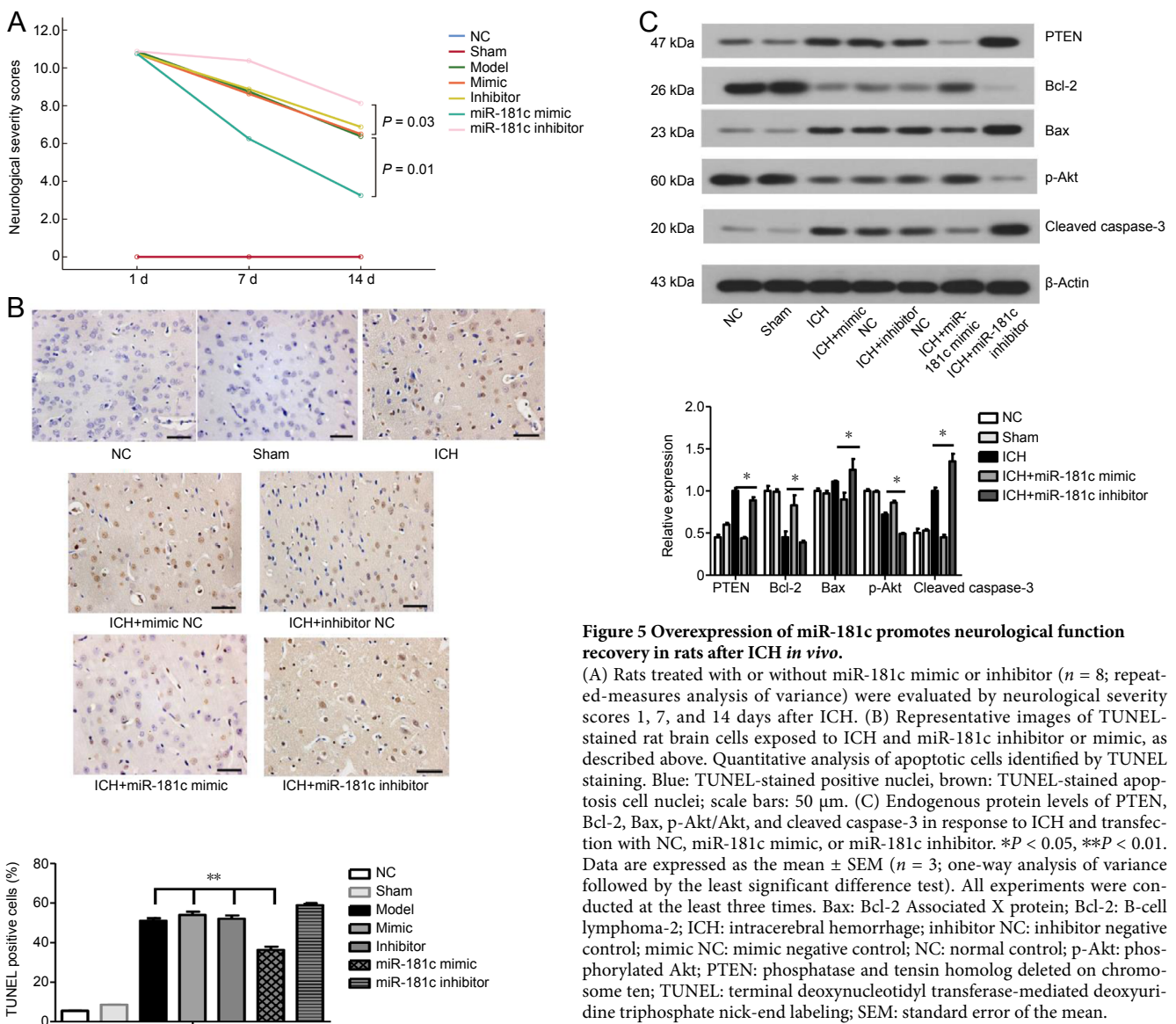
Figure 5 Overexpression of miR-181c promotes neurological function recovery in rats after ICH *in vivo*.
(A) Rats treated with or without miR-181c mimic or inhibitor ($n = 8$; repeated-measures analysis of variance) were evaluated by neurological severity scores 1, 7, and 14 days after ICH. (B) Representative images of TUNEL-stained rat brain cells exposed to ICH and miR-181c inhibitor or mimic, as described above. Quantitative analysis of apoptotic cells identified by TUNEL staining. Blue: TUNEL-stained positive nuclei, brown: TUNEL-stained apoptosis cell nuclei; scale bars: 50 μm. (C) Endogenous protein levels of PTEN, Bcl-2, Bax, p-Akt/Akt, and cleaved caspase-3 in response to ICH and transfection with NC, miR-181c mimic, or miR-181c inhibitor. ∗$P < 0.05$, ∗∗$P < 0.01$. Data are expressed as the mean ± SEM ($n = 3$; one-way analysis of variance followed by the least significant difference test). All experiments were conducted at the least three times. Bax: Bcl-2 Associated X protein; Bcl-2: B-cell lymphoma-2; ICH: intracerebral hemorrhage; inhibitor NC: inhibitor negative control; mimic NC: mimic negative control; NC: normal control; p-Akt: phosphorylated Akt; PTEN: phosphatase and tensin homolog deleted on chromosome ten; TUNEL: terminal deoxynucleotidyl transferase-mediated deoxyuridine triphosphate nick-end labeling; SEM: standard error of the mean.

Zhou K, Zhong Q, Wang YC, Xiong XY, Meng ZY, Zhao T, Zhu WY, Liao MF, Wu LR, Yang YR, Liu J, Duan CM, Li J, Gong QW, Liu L, Yang MH, Xiong A, Wang J, Yang QW (2017) Regulatory T cells ameliorate intracerebral hemorrhage-induced inflammatory injury by modulating microglia/macrophage polarization through the IL-10/GSK3beta/PTEN axis. J Cereb Blood Flow Metab 37:967-979.

Zhuang L, Qu H, Cong J, Dai H, Liu X (2019) MiR-181c affects estrogen-dependent endometrial carcinoma cell growth by targeting PTEN. Endocr J 66:523-533.

Zille M, Karuppagounder SS, Chen Y, Gough PJ, Bertin J, Finger J, Milner TA, Jonas EA, Ratan RR (2017) Neuronal death after hemorrhagic stroke in vitro and in vivo shares features of ferroptosis and necroptosis. Stroke 48:1033-1043.